Phase Stability of Nickel Hydroxides and Oxyhydroxides

A. Van der Ven,[a,z] D. Morgan,[b] Y. S. Meng,[c] and G. Ceder[c,*]

[a]*Department of Materials Science and Engineering, University of Michigan, Ann Arbor, Michigan 48109, USA*
[b]*Department of Materials Science and Engineering, University of Wisconsin, Madison, Wisconsin 53706, USA*
[c]*Department of Materials Science and Engineering, Massachusetts Institute of Technology, Cambridge, Massachusetts 02139, USA*

We investigate phase stability of several nickel hydroxides from first-principles. Hydrogen removal from β-Ni(OH)$_2$ is predicted to occur through a biphasic reaction to β-NiOOH involving a change in the stacking sequence from T1 [for β-Ni(OH)$_2$] to P3 (for β-NiOOH). Further topotactic removal of hydrogen from β-NiOOH can only occur after a step in a range between 0.4 and 0.9 V is surpassed. We also propose an energetically stable crystal structure for stoichiometric γ-NiOOH, which offers an explanation for the oxidation limit of 3.66 for Ni. In this structure, potassium in the intercalation layer resides halfway between adjacent trigonal prismatic sites. We conclude with a discussion of the role of the electrolyte in determining phase stability as well as the voltage profile of γ-NiOOH.
© 2005 The Electrochemical Society. [DOI: 10.1149/1.2138572] All rights reserved.

Nickel hydroxide compounds are widely used as cathodes in primary and secondary alkaline batteries. Several different forms of nickel hydroxide exist, each differing in crystal structure and composition. Important nickel hydroxide variants are referred to as β-NiOOH, β-Ni(OH)$_2$, γ-NiOOH, and α-Ni(OH)$_2$. During charge and discharge, a variety of phase transformations can occur between the different nickel hydroxide variants. The Bode diagram (Fig. 1)[1] qualitatively captures most of the essential phase transformations in Ni hydroxide electrodes. Charging of β(II) nickel hydroxide Ni(OH)$_2$ leads to β(II) nickel oxyhydroxide NiOOH. Ni in β(II)–Ni(OH)$_2$ has a valence of +2 while Ni in β(III)–NiOOH has a valence of +3. The β(III)–NiOOH compound can either be discharged back to Ni(OH)$_2$, or it can be charged even further, transforming to γ-NiOOH, a phase that is poorly characterized but is nevertheless known to contain water molecules and potassium which are drawn from the alkaline electrolyte.[2] Upon discharge, the γ phase transforms under most conditions to an α-Ni(OH)$_2$ which, like γ, also contains water molecules along with other molecules from the electrolyte or air, such as CO$_3^{2-}$ or NH$_2^-$.[2] Electrochemical cycling can occur over the γ → α transformation, but α usually transforms to β(II) after some time. γ-NiOOH has also been observed to transform directly to β(II)–Ni(OH)$_2$ upon discharge, bypassing the α phase.[3]

Although the general features of Ni-hydroxide-based electrode materials have been characterized over the last century,[1,2,4] many of their basic properties remain unknown. Important questions persist about the precise crystal structures of γ-NiOOH and β-NiOOH. Furthermore, the relationship between the crystal structures of β and γ-NiOOH and their measured capacities are still unclear. While it has not been possible to extract more than one electron per Ni ion in the β-Ni(OH)$_2$ to β-NiOOH couple, more than one electron per Ni can be cycled if the γ phase participates in the couple. Oxidation of the γ phase has, however, been limited to a maximum oxidation state for Ni of +3.66,[5,6] although the reason for this limitation is not understood. Further oxidation of γ by either chemical or electrochemical means might produce an electrode capable of cycling two electrons per Ni, thereby significantly enhancing the capacity of alkaline cells. Cycling of Ni^{2+} to Ni^{4+} has been demonstrated in Li-ion batteries.[7]

In this paper, we investigate the phase stability of nickel hydroxides from first-principles. We predict that the previously uncharacterized crystal structure of β(III)–NiOOH is actually derived from the P3 host. Furthermore, we identify a plausible crystal structure for the γ-NiO$_2$(H$_2$O)$_{0.67}$K$_{0.33}$H$_x$ phase that is consistent with available experimental observations. The proposed crystal structure has a P3 host and the K ions reside exactly between adjacent trigonal prismatic sites of the intercalation layer. We have also calculated the topotactic voltage curves for the β and γ phases, and predict the existence of a large step in voltage at β-NiOOH, which effectively limits the capacity of the β Ni-hydroxide compound to one electron per Ni ion.

Methodology

We combine first-principles electronic structure calculations with a cluster expansion approach for the disorder of protons in the materials to calculate phase stability and thermodynamic properties of the nickel hydroxide system. The electronic structure calculations yield information about solids at zero Kelvin, including energy differences between different crystal structures, equilibrium lattice parameters, and electronic charge densities. For solids exhibiting configurational disorder (e.g., resulting from the many possible arrangements of hydrogen atoms and vacancies within the hydroxide host structures at nonstoichiometric compositions), the energies calculated with electronic structure methods can be combined with a lattice model formalism (i.e., the cluster expansion) and Monte Carlo simulations to obtain finite temperature thermodynamic properties such as phase diagrams and voltage curves. This approach has been successfully applied to study phase stability in a wide variety of oxides, and we refer the reader to the following references for more details.[8-11]

The energies calculated with electronic structure methods were performed in the generalized gradient approximation (GGA) to density functional theory using the pseudopotential method. While this is one of the most accurate first-principles approaches, documented problems on transition metal oxides exist.[12,9] Nevertheless, based on our previous work on Li$_x$CoO$_2$ and Li$_x$NiO$_2$,[8-10] we do not believe these would affect the outcome of our findings, which focus on determining relative stabilities and qualitative variations in voltage profiles with hydrogen concentration. The particular numerical implementation used for this work was a plane-wave projector augmented wave (PAW)[13,14] pseudopotential method as coded in the Vienna Ab-initio Simulation Package (VASP).[15] All calculations were spin polarized initialized with ferromagnetic magnetization.

Phase Stability of β-H$_x$NiO$_2$

The transformation from β(II)–Ni(OH)$_2$ to β(III)–NiOOH upon charging of the nickel hydroxide compound is well known to be a

---

* Electrochemical Society Active Member.
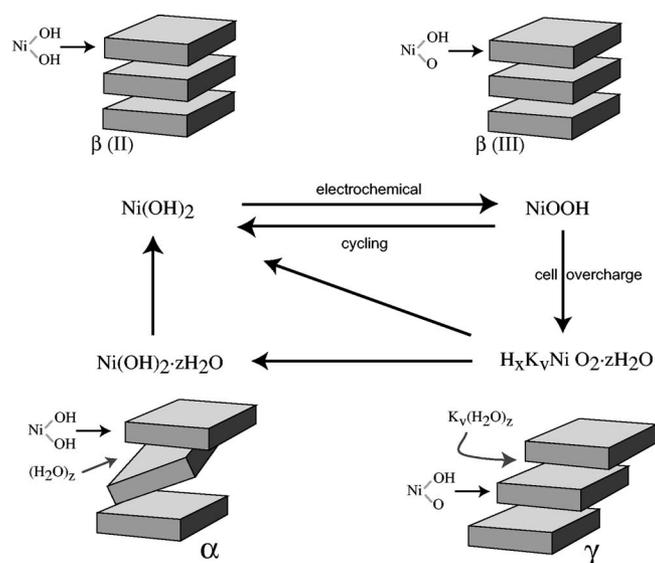z E-mail: avdv@unich.edu

Figure 1. The Bode diagram illustrating the different variants of Ni-hydroxide and the possible phase transformations between them.

Figure 2. The crystal structures of β-Ni(OH)$_2$ having the T1 oxygen stacking sequence (ABAB) and β-NiOOH having the P3 oxygen stacking sequence (AABBCC). Also shown (right) is local coordination of hydrogen (small circles) by oxygen (large circles).

biphasic reaction.[16] While the crystal structure of β(II)–Ni(OH)$_2$ is isomorphic with CdI$_2$ (which has the T1 stacking sequence), that of β(III)–NiOOH has not been characterized.[2,3] The crystal structure of β-Ni(OH)$_2$ consists of close-packed oxygen planes with an ABAB stacking sequence.[2] The Ni atoms occupy octahedral sites between alternating oxygen layers, and the hydrogen atoms reside in the tetrahedral sites of the remaining layers between oxygen. The hydrogen atoms do not reside at the centers of the tetrahedral sites but are tightly bound to one of the four oxygen atoms surrounding the tetrahedral sites as illustrated in Fig. 2. For convenience, we will also write β-Ni(OH)$_2$ as β-H$_2$NiO$_2$, which upon removal of hydrogen during charging becomes β-H$_x$NiO$_2$ with x ranging between 0 and 2. Written in this form, it becomes clear that β nickel hydroxide consists of a rigid NiO$_2$ host (which can undergo structural transformations) and removable H atoms that occupy interstitial sites within the host.

The phases that are thermodynamically stable and appear in equilibrium for the H$_x$NiO$_2$ system as a function of hydrogen concentration are those with the lowest Gibbs free energy. Free energies of oxide compounds such as the β-Ni-hydroxides can be calculated by combining first-principles electronic structure methods with tools from statistical mechanics (cluster expansion combined with Monte Carlo simulations).[8-10] To this end, we calculated the energy of a variety of different hydrogen-vacancy arrangements (eight configurations) over the tetrahedral sites of the T1 host structure of NiO$_2$ for hydrogen concentrations ranging from $x = 0$ to 2 within GGA using the PAW pseudopotential method. We also calculated the energy of different hydrogen arrangements within the P3 host structure of NiO$_2$ (six configurations). This host structure consists of an AAB-BCC oxygen stacking sequence, which can be derived from the T1 ABAB stacking sequence by gliding the O–Ni–O slabs of T1 with respect to each other to yield an AA stacking sequence across the intercalation layer (where hydrogen resides). As in T1-NiO$_2$, the Ni ions in the P3 structure reside in octahedral sites between oxygen planes with an AB stacking sequence. We considered the P3 host structure in addition to that of T1 for two reasons: (*i*) it is observed to be the crystal structure of β-CoOOH;[17] (*ii*) the AA oxygen stacking sequence across the intercalation layers allows hydrogen atoms to form strong primary and secondary hydrogen bonds with oxygen atoms as illustrated in Fig. 2.

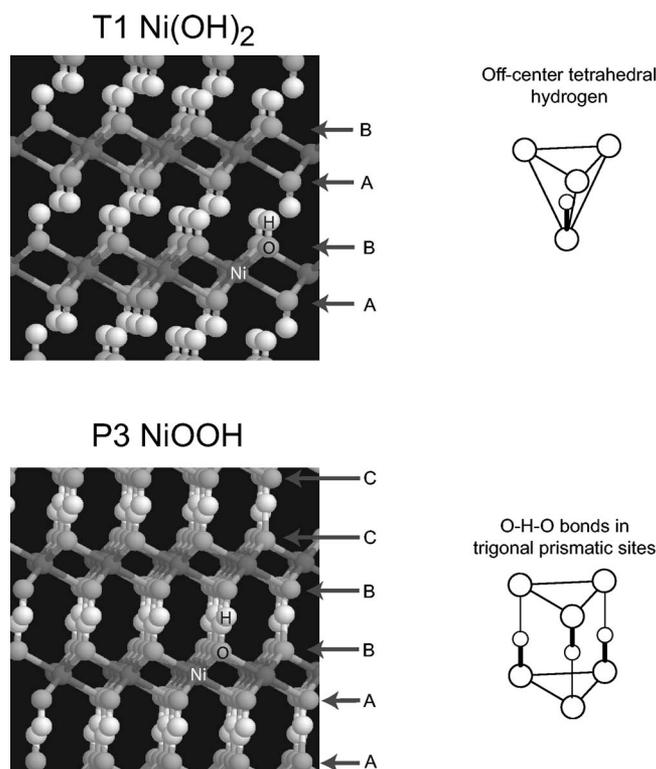The calculated energies for different arrangements in T1 and P3 H$_x$NiO$_2$ were used to parameterize the interaction parameters of lattice models (i.e., cluster expansions), one for each host structure (five interaction parameters for the cluster expansion of the T1 host, and six interaction parameters for the cluster expansion of the P3 host), which were then combined with Monte Carlo simulations to calculate finite temperature Gibbs free energy curves. Figure 3 illustrates calculated free energies of β-H$_x$NiO$_2$ at room temperature. As is clear from Fig. 3, the T1 crystal structure is not the most favored thermodynamically, as hydrogen is extracted from β-Ni(OH)$_2$. Instead, the free energy of the solid is lowered if it phase separates
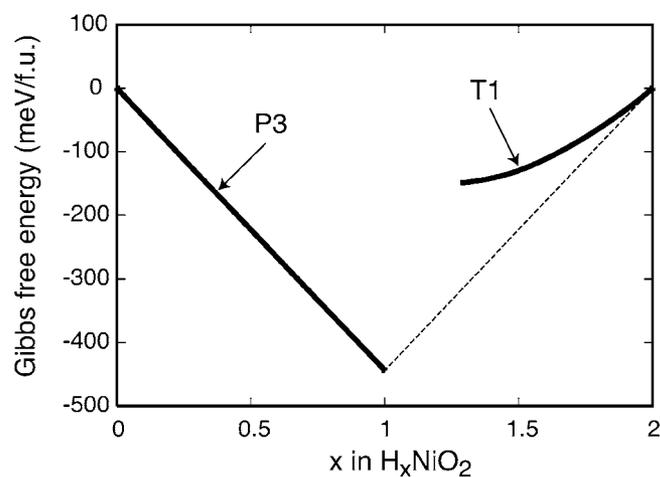

Figure 3. Calculated Gibbs free energies for the T1 and P3 forms of H$_x$NiO$_2$. The dashed line corresponds to the common between the T1 and P3 free energy curves and signifies a two-phase coexistence region between Ni(OH)$_2$ and NiOOH.

into a two-phase mixture of T1 having stoichiometry $Ni(OH)_2$ and a phase with crystal structure P3 having stoichiometry NiOOH. The free energy of this two-phase mixture is given by the common tangent (dashed line in Fig. 3) to the free energies of T1 at $x = 2$ and P3 at $x = 1$. Hence, the first-principles calculations predict that P3 NiOOH forms through a biphasic reaction from T1 upon charge.

While not evident from the free energy curves in Fig. 3, our first-principles calculations not only indicate that P3 $HNiO_2$ is more stable than T1 $HNiO_2$, but that T1 $HNiO_2$ is actually dynamically unstable, and spontaneously transforms to P3 without encountering an energy barrier. We found that several of the ordered hydrogen-vacancy arrangements we considered at $x = 1$ make the T1 host structure of NiO_2 dynamically unstable, inducing a spontaneous change in the stacking sequence of the oxygen layers from an ABAB sequence to the AABBCC sequence of P3.

The relative stability between T1 and P3 $HNiO_2$ (i.e., NiOOH) can be directly attributed to the local environment of the hydrogen atoms within the intercalation layers. While T1 and P3 have identical O–Ni–O slabs, crucial differences exist between their stacking sequences across the H intercalation layer. In the P3 crystal structure, the oxygen atoms directly face each other across the intercalation plane as illustrated in Fig. 2. This makes it possible for the hydrogen atoms to tightly bind to one of the oxygen atoms of one O–Ni–O slab (covalent bond with a calculated length of ~ 1.1 Å) and to form an energetically favorable hydrogen bond with the oxygen atom of the adjacent O–Ni–O slab (with a calculated bond length of ~ 1.4 Å). The ability to form a secondary hydrogen bond is absent in the T1 crystal structure, making it energetically unfavorable compared to P3 once hydrogen is removed from $Ni(OH)_2$. Within the tetrahedral sites of T1, the H forms a covalent bond with one oxygen atom (with calculated bond length of ~ 1 Å) but is too far (~ 2.3 Å) from its three other nearest-neighbor oxygen atoms to form any favorable secondary hydrogen bonds. The T1 structure only forms at $x = 2$ in H_xNiO_2, because the P3 structure does not have enough H sites to accommodate the two hydrogen atoms per formula unit.

Because the Gibbs free energy contains all relevant thermodynamic properties of a system at constant pressure and temperature, other thermodynamic properties such as the intercalation voltage can also be obtained in a straightforward manner. In fact, the voltage is linearly related to the chemical potential of hydrogen within H_xNiO_2 and the chemical potential is proportional to the slope of the free energy curves illustrated in Fig. 3. Figure 4 illustrates the predicted voltage profile of H_xNiO_2 as the hydrogen content is varied. While the relative variation of the voltage is well predicted from first-principles, there is currently no accurate methodology to calculate reference states for hydrogen. Hence, the absolute value of the voltage cannot be predicted from first-principles. To facilitate comparison with experiment, we shifted all calculated voltages by a constant such that the predicted voltage of the NiOOH → $Ni(OH)_2$ couple is set to zero. Then for any specific anode, the voltage curve of Fig. 4 can be shifted uniformly by an amount that is equal to the equilibrium open-cell voltage measured during the $\beta(III) \rightarrow \beta(II)$ couple. The plateau between $x = 1$ and 2 corresponds to the voltage of the biphasic reaction as T1 $Ni(OH)_2$ transforms to P3 NiOOH upon charge, or the reverse reaction upon discharge. (There is no polarization between calculated charge and discharge voltages because the solid lines represent the open-circuit voltage at complete equilibrium.)

The predicted voltage profile for the β structure exhibits a large step at $x = 1$ close to 0.9 V. This step arises from the energetic stability of the P3 crystal structure of β-NiOOH in which the hydrogen atoms can form energetically favorable O–H–O bonds as illustrated in Fig. 2. Further removal of hydrogen from P3 NiOOH would require breaking these energetically favorable bonds. A sizable increase in voltage is therefore necessary to remove hydrogen from P3 β-NiOOH. We note that predicted voltages are often modified when treating electron correlation in the DFT + U method.[12,18]
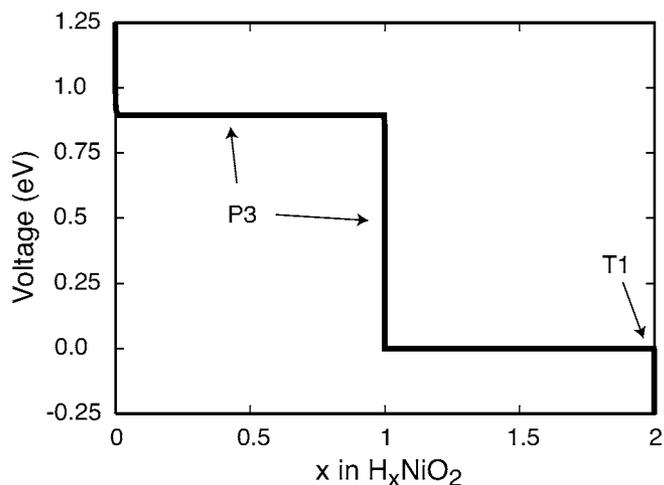

Figure 4. Calculated equilibrium voltage curve for β nickel hydroxide within the GGA approximation (the GGA + U approximation predicts a smaller voltage step of close 0.4 V). The reference state for the anode has been arbitrarily chosen such that the plateau corresponding to the $\beta(II) \leftrightarrow \beta(III)$ couple is zero. To compare to experiment, the whole curve should be shifted by an amount equal to the measured voltage for the $\beta(II) \leftrightarrow \beta(III)$ couple.

Using GGA + U with U values between 3 and 6 eV predicts a step of around 0.4 V at $x = 1$ as compared to 0.9 V calculated with GGA. We expect the actual voltage step to be somewhere between these two values. A voltage step between 0.4 and 0.9 eV, needed to oxidize Ni beyond +3 in this structure, makes it unlikely that substantially more capacity will be obtained from the β phase with aqueous electrolytes. It is, however, possible that further charging at lower potential is possible by conversion of the β phase to another phase (such as γ).

The γ-NiOOH Phase

The γ-NiOOH phase represents a family of Ni-hydroxide compounds characterized by a large interlayer sheet distance.[2] The general chemical formula of the γ form can be written as $H_xA_y(H_2O)_zNiO_2$ in which A is typically Na or K and y and z are often claimed to be 0.33 and 0.66, respectively.[2,19] A common form[2,5] of γ is $H_xK_{0.33}(H_2O)_{0.66}NiO_2$, which can be obtained by overcharging β-NiOOH. The potassium and water come from the electrolyte according to a reaction such as

$$3(\beta - NiOOH) + KOH + H_2O \rightarrow H_2K(H_2O)_2Ni_3O_6$$
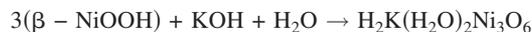
The crystal structure of γ-$H_xK_{0.33}(H_2O)_{0.66}NiO_2$ is poorly characterized, though it is known that γ has a P3 oxygen stacking sequence[2] similar to that predicted in this work for β-NiOOH. Furthermore, experimental evidence suggests that the maximal oxidation state of Ni in the γ phase is +3.66.[2,5,6]

Starting with the stoichiometric chemical formula for γ (namely, $H_xK_{0.33}(H_2O)_{0.66}NiO_2$), we used first-principles total energy calculations to determine an energetically stable crystal structure for this phase. An energetically stable form of $H_xK_{0.33}(H_2O)_{0.66}NiO_2$ is illustrated in Fig. 5, which shows both a projection (along the direction perpendicular to the close-packed oxygen planes) and a side view of the intercalation layer of the crystal structure. The structure has an AABBCC oxygen stacking sequence as in P3, which is consistent with what has been observed experimentally. The K atoms, which are ordered in a $\sqrt{3a} \times \sqrt{3a}$ superlattice, do not reside at the center of a prismatically coordinated (by oxygen) interstitial site but instead reside at the center of a rectangle of oxygen atoms, two belonging to the O–Ni–O slab above and two belonging to the O–Ni–O slab below. In this way, K atoms avoid sites that share faces with Ni either from above or below the intercalation layer. The
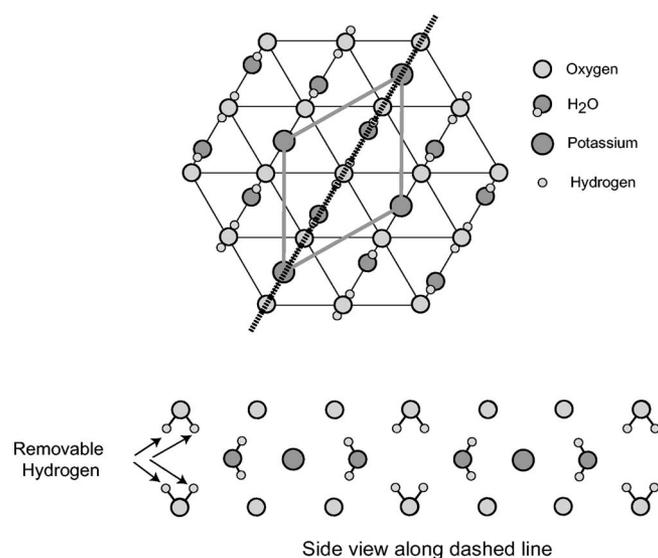
Figure 5. Intercalation layer of proposed crystal structure for γ-NiOOH. The proposed structure for γ-NiOOH has a P3 oxygen stacking sequence with Ni residing in octahedral sites.

Figure 6. Calculated topotactic voltage curve of γ-NiOOH within the GGA approximation. The reference state for the anode is the same as that used in Fig. 4.

water molecules are oriented such that the vector connecting the two H atoms of each water molecule is perpendicular to the O–Ni–O slabs.

It is likely that the K and water molecules behave as inert components during topotactic (i.e., without changing the structure) charging and discharging of the γ-phase. In that case, the other hydrogen atoms which are bound to oxygen atoms of the O–Ni–O slabs can be removed from the γ crystal structure. These hydrogen atoms are indicated by arrows in Fig. 5. There are four active hydrogen sites for every three Ni atoms. This means that x in the stoichiometric formula for γ-$H_xK_{0.33}(H_2O)_{0.66}NiO_2$ can only range from 0 to 1.33. When $x = 0$, the valence of Ni is +3.66. When $x = 1.33$, the valence of Ni is +2.33. When half the active hydrogen sites are filled, the valence of Ni is exactly +3. In this proposed γ crystal structure, it is clearly crystallographic factors that impose the seemingly artificial bound of +3.66 on the maximum oxidation state of the Ni atoms. This suggests that higher Ni valence states, and associated larger cathode capacities, might be realized through structural modification.

The proposed crystal structure for γ illustrated in Fig. 5 has a monoclinic unit cell and belongs to the *C2/m* space group. Table I lists calculated lattice parameters [calculated at $x = 0.66$ in $H_xK_{0.33}(H_2O)_{0.66}NiO_2$] along with the calculated coordinates of the asymmetric unit cell for the atoms of the crystal (taken from calculations at $x = 1.33$ in $H_xK_{0.33}(H_2O)_{0.66}NiO_2$ where all hydrogen

sites are filled). We emphasize that we have only demonstrated that this structure for γ-NiOOH is locally stable (i.e., it is mechanically stable against deformation into another structure). The arrangement of hydrogen, potassium, and water molecules between the O–Ni–O slabs may only correspond to a local minimum in energy and not a global minimum. Nevertheless, while we have not exhausted all possible hydrogen, potassium, and water arrangements within the intercalation layer, the proposed crystal structure is consistent with what is currently known about the γ-phase. The monoclinic symmetry of the structure of Fig. 5 and Table I results from the superlattice ordering of the K and water molecules in the intercalation layer. In real crystals, however, it is likely that the K and water molecules of γ-NiOOH are not perfectly ordered but instead exhibit short-range order that is similar to that in Fig. 5 on a local level. In that case, the symmetry of the crystal adopts that of the host structure, which for the P3 stacking is $R\bar{3}m$ symmetry. An important feature of this crystal structure is that the K atoms do not reside in a trigonal prismatic site of the intercalation layer of the P3 host but rather reside exactly between adjacent trigonal prismatic sites.

Because the formation of γ upon overcharging or oxidizing of β-NiOOH is accompanied by the uptake of K and H_2O, and because discharging of γ proceeds through a transformation to α or β-$Ni(OH)_2$, it is experimentally difficult (if not impossible) to isolate the topotactic voltage profile for the γ phase. With first-principles computational tools, calculating a topotactic voltage profile is straightforward. Figure 6 illustrates the topotactic voltage profile for the proposed structure of stoichiometric γ-$H_xK_{0.33}(H_2O)_{0.66}NiO_2$ as the hydrogen content is varied from $x = 0$ to 1.33. The voltage curve was calculated with Monte Carlo simulations applied to a lattice model Hamiltonian (six interaction terms) that was fit to GGA first-principles energies of seven hydrogen-vacancy arrangements in the γ-$K_{0.33}(H_2O)_{0.66}NiO_2$ host. The same reference state for the anode was used as for the β couple. Two plateaus are predicted, separated by a step of almost 1 V at $x = 0.66$ (corresponding to a Ni valence state of +3). The step in the voltage profile is not observed experimentally, as γ never discharges topotactically but rather transforms to either β or α. The voltage plateau between $x = 0$ and 0.66 could potentially be observed when γ is charged beyond a Ni oxidation state of +3.

In our calculations several approximations were made. These include the neglect of hydrogen vibrational degrees of freedom and the vibrational zero point energies. While vibrational degrees of

---

Table I. Calculated lattice parameters and asymmetric unit cell for the proposed γ crystal structure. The proposed structure has a monoclinic unit cell (doubly primitive, face centered) and belongs to the *C2/m* space group. The first set of H sites has partial occupancy as x is varied in $H_xK_{0.33}(H_2O)_{0.66}NiO_2$.

$a = 5.1$ $b = 9.1$ $c = 6.84$ $\alpha = 90.0$ $\beta = 105.7$ $\gamma = 90.0$
H 8j ($x = 0.4042$ $y = 0.0802$ $z = 0.3435$)
H 8j ($x = 0.4620$ $y = 0.2643$ $z = 0.3651$)
K 2d (0 0 1/2)
Ni 2a (0 0 0)
4g (0 $y = 0.2891$ 0)
O 4h (0 $y = 0.2939$ 1/2)
4i ($x = 0.3739$ 0 $z = 0.2491$)
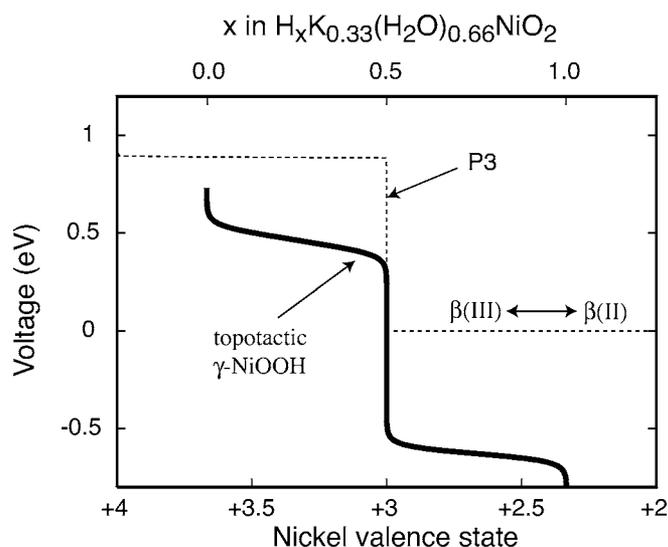8j ($x = 0.3718$ $y = 0.6564$ $z = 0.1480$)

freedom can safely be ignored for most elements, they are important for hydrogen. Because of this, the voltages predicted for the two voltage plateaus are only approximate and quantitative comparisons with experiment must be avoided. Furthermore, the topotactic voltage profile of Fig. 6 is for a stoichiometric γ phase with exactly 0.33 K and 0.66 H_2O molecules in the intercalation layers. In the experiment, the potassium and water contents may deviate from these stoichiometric values which will also change the voltage.

Discussion

Our first-principles study of phase stability in the H_xNiO_2 system predicts that β-NiOOH has a different oxygen stacking sequence than β-Ni(OH)$_2$. β-NiOOH is stable in the P3 structure with an AABBCC oxygen stacking sequence, while β-Ni(OH)$_2$ is stable in the T1 host with ABAB stacking sequence. This has important implications for the β(II) → β(III) transformation, as it requires a reshuffling of the oxygen planes across the intercalation layers. One mechanism by which such structural phase transformations can occur is by passage of dislocations through the intercalation layers.[20] The work by Delmas et al.[19] suggests, however, that this may not be the dominant mechanism to kinetically facilitate the β(II) → β(III) transformation. They showed that oxidation of Ni(OH)$_2$ leads to a NiOOH compound having an amorphous-like X-ray diffraction pattern (XRD), which nevertheless, reverts back to a crystalline form of Ni(OH)$_2$ upon reduction. While passage of dislocations to facilitate the β(II) → β(III) transformation will introduce structural defects which could conceivably lead to an amorphization of the host structure, the damage resulting from dislocation passage is irreversible and is unlikely to be removed upon reduction of NiOOH to Ni(OH)$_2$. Instead, the mechanism by which the β(II) → β(III) transformation actually proceeds may be linked to the occurrence of noncooperative Jahn-Teller distortions of the oxygen octahedra around the Ni ions, observed by Delmas et al.[19] in NiOOH. Such noncooperative Jahn-Teller distortions in NiOOH can locally accommodate the strain induced by the stacking sequence change during the β(II) → β(III) transformation, and because the strain accommodation is local, the stacking sequence shifts need not be cooperative over long distance, leading to a structure that may appear amorphous with XRD measurements. We note that in our GGA pseudopotential calculations, we were unable to stabilize a cooperative Jahn-Teller distortion in the P3 form of NiOOH.

An important prediction in this work is the large voltage step at $x = 1$ in H_xNiO_2. This step, which arises from the strong hydrogen bonds with oxygen in the P3 NiOOH crystal structure (Fig. 2), essentially limits the capacity of β Ni-hydroxide compounds to one electron per Ni in conventional aqueous electrolytes. A step in the voltage profile between 0.4 and 0.9 V is unlikely to be eliminated by chemical substitution. In aqueous electrolytes, further charge of β-NiOOH leads to a transformation to the γ phase which forms upon uptake of potassium and water.[2] Only with nonaqueous electrolytes is it conceivable that the full topotactic H_xNiO_2 voltage curve (with x ranging between 0 and 2) can be realized in an electrochemical cell.

With a detailed crystallographic model for γ-$H_xK_{0.33}(H_2O)_{0.66}NiO_2$, it is possible to calculate a topotactic voltage curve. Our calculations suggest that the topotactic voltage curve for this crystal structure consists of two plateaus separated by a step approaching 1 V at a hydrogen concentration corresponding to a Ni valence state of +3. In experiment, it is unlikely that a topotactic voltage curve for γ-NiOOH can be isolated, as the formation of γ and its subsequent two-phase equilibria with either a β or α nickel hydroxide involves the insertion or removal not only of hydrogen but also potassium and water molecules from the electrolyte.

It is the ability of both the γ and α nickel hydroxides to exchange atoms and molecules with the electrolyte that sets these phases apart from most other intercalation compounds. The fact that these phases can exchange components with the electrolyte during charge and discharge means that their voltage depends not only on the state of
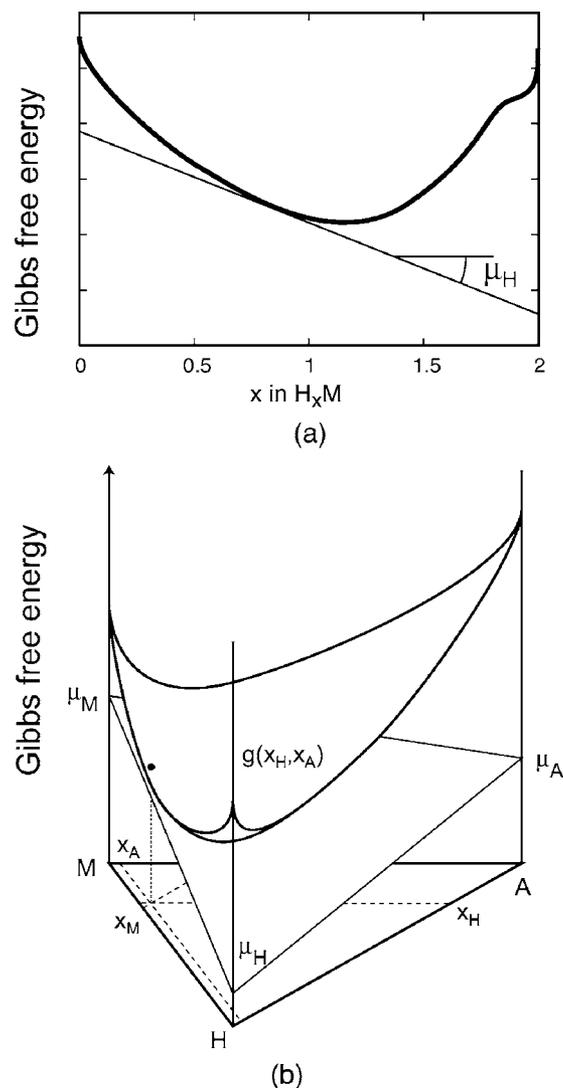

Figure 7. Schematic Gibbs free energies for topotactic intercalation (a) and intercalation accompanied by mass exchange with the electrolyte (b). M corresponds to the host, H to hydrogen, and A to a species of the electrolyte that can be incorporated within the host during charge and discharge.

charge, but also on the thermodynamic state of the electrolyte. For intercalation compounds such as β-H_xNiO_2, which do not exchange species with the electrolyte, the equilibrium voltage of the compound at fixed temperature (and for a fixed anode) is a function only of the overall hydrogen concentration in the compound. Indeed, the voltage is linearly related to the chemical potential of hydrogen within the compound, which is equal to the slope of the Gibbs free energy of the host with respect to x, as illustrated schematically in Fig. 7a. This slope is independent of the composition of the electrolyte.

Compounds that are able to exchange matter with the electrolyte tend to equilibrate with the electrolyte. The hydrogen chemical potential and hence the voltage for such compounds is affected by the equilibrium reached between the cathode and the electrolyte. While a compound such as γ-NiOOH can exchange several species with the electrolyte, the basic principles can be illustrated with a simple hypothetical compound that only exchanges one component with the electrolyte. Figure 7b illustrates a Gibbs free energy plot for a host structure M that can intercalate hydrogen, H; and simultaneously absorb species A from the electrolyte. The chemical potentials μ_A, μ_H, and μ_M for the different species at a given mole fraction x_A and

x_H are determined by the intercept of the plane tangent to the Gibbs free energy curve at x_A and x_H with the axes $x_A = 1$, $x_H = 1$, and $x_M = 1$, respectively.

The chemical potential of A in the electrolyte is determined by the overall composition of the electrolyte. An increase in the composition of A in the electrolyte, holding all other species constant, leads to an increase in the chemical potential of A. (It is customary to speak of the activity of a component of the electrolyte instead of its chemical potential, the former being proportional to the exponential of the latter.) If the intercalation compound is in equilibrium with the electrolyte (with respect to exchange of A), then the composition of A in the intercalation compound at fixed state of charge (i.e., H composition) must be such that the plane tangent to the Gibbs free energy of the host intersects the $x_A = 1$ axis at $\mu_A = \mu_A^{electrolyte}$. Hence, the chemical potential of A in the electrolyte and the state of charge determine the equilibrium concentration of A in the intercalation compound. Figure 7b also illustrates that in general, as the state of charge (i.e., hydrogen concentration) varies, the equilibrium concentration of A in the compound will change as well. Furthermore, and more importantly, a change in the chemical potential of A in the electrolyte will result in a different voltage profile, as the hydrogen chemical potential of the compound depends on $\mu_A = \mu_A^{electrolyte}$. This illustrates that the voltage of compounds such as γ and α nickel hydroxide can be tailored not only by chemical modification of the compound itself (through chemical substitution of the compound, for example), but also by modifying the electrolyte. For γ and α nickel hydroxide, the equilibrium with the electrolyte is more complicated than schematically illustrated in Fig. 7b, as several species can be exchanged with the electrolyte, thereby precluding any graphical representation of such equilibrium. However, the principles are the same as those illustrated in Fig. 7b, and the more complex equilibrium problem could be studied with general electrolyte solution theory.

Conclusion

We have investigated phase stability among several variants of Ni-hydroxide from first-principles. Our calculations within the GGA predict that β-Ni(OH)$_2$, stable in the T1 crystal structure, transforms upon charging through a biphasic reaction to β-NiOOH having a P3 crystal structure. Hence, the calculations predict that in thermodynamic equilibrium, β-NiOOH has a host structure with a different oxygen-stacking sequence from that of β-Ni(OH)$_2$, which points

attention to the importance of defects in the material to facilitate the transformation and reduce hysteresis between charge and discharge. The calculations also predict that further hydrogen removal from β-NiOOH is unlikely with aqueous electrolytes and with retention of the structure. We have also proposed an energetically stable crystal structure for γ-NiOOH which is consistent with available experimental evidence, and which offers a crystallographic explanation for the oxidation limit of 3.66 for Ni in these compounds.

References

1. H. Bode, K. Dehmelt, and J. Witte, *Electrochim. Acta*, **11**, 1079 (1966).
2. P. Oliva, J. Leonardi, J. F. Laurent, C. Delmas, J. J. Braconnier, M. Figlanz, F. Fievet, and A. De Guibert *J. Power Sources*, **8**, 229 (1982).
3. F. Barde, M. R. Palacin, Y. Chabre, O. Isnard, and J. M. Tarascon, *Chem. Mater.*, **16**, 3936 (2004).
4. F. Barde, M. R. Palacin, B. Beaudoin, and J. M. Tarascon, *Chem. Mater.*, **17**, 470 (2005).
5. D. A. Corrigan and S. L. Knight, *J. Electrochem. Soc.*, **136**, 613 (1989).
6. J. DeSilvestro, D. A. Corrigan, and M. J. Weaver, *J. Electrochem. Soc.*, **135**, 885 (1988).
7. J. Reed and G. Ceder, *Electrochem. Solid-State Lett.*, **5**, A145 (2002).
8. A. Van der Ven, M. K. Aydinol, G. Ceder, G. Kresse, and J. Hafner, *Phys. Rev. B*, **58**, 2975 (1998).
9. M. E. A. Y. de Dompablo, A. Van der Ven, and G. Ceder, *Phys. Rev. B*, **66**, 064112 (2002).
10. D. Carlier, A. Van der Ven, C. Delmas, and G. Ceder, *Chem. Mater.*, **15**, 2651 (2003).
11. G. Ceder, A. Van der Ven, C. Marianetti, and D. Morgan, *Modell. Simul. Mater. Sci. Eng.*, **8**, 311 (2000).
12. F. Zhou, M. Cococcioni, C. A. Marianetti, D. Morgan, and G. Ceder, *Phys. Rev. B*, **70**, 235121 (2004).
13. P. E. Blochl, *Phys. Rev. B*, **50**, 17953 (1994).
14. G. Kresse and D. Joubert, *Phys. Rev. B*, **59**, 1758 (1999).
15. G. Kresse and J. Furthmuller, *Comput. Mater. Sci.*, **6**, 15 (1996).
16. C. Leger, C. Tessier, M. Menetrier, C. Denage, and C. Delmas, *J. Electrochem. Soc.*, **146**, 924 (1999).
17. M. Butel, L. Gautier, and C. Delmas, *Solid State Ionics*, **122**, 271 (1999).
18. M. Cococcioni and S. de Gironcoli, *Phys. Rev. B*, **71**, 035105 (2005).
19. A. Demourgues, L. Gautier, A. V. Chadwick, and C. Delmas, , *Nucl. Instrum. Methods Phys. Res. B*, **133**, 39 (1997).
20. H. Gabrisch, R. Yazami, and B. Fultz, *Electrochem. Solid-State Lett.*, **5**, A111 (2002).